MODELLING AND TESTING OF AN ERF VIBRATION DAMPER FOR LIGHT ROTORS WITH LARGE AMPLITUDES

Jens Bauer, bauer@sdy.tu-darmstadt.de
Institute of Structural Dynamics, Technische Universität Darmstadt, Germany
Gregory Bregion Daniel, gbdaniel@fem.unicamp.br
Faculty of Mechanical Engineering, University of Campinas, Brazil

Abstract. *Vibrations in rotating machines can often be suppressed by the passive methods of damping or detuning. For systems with different rotational speeds or shifting system parameters (bearing stiffness or mass), the passive methods are no longer the best choice. Using active or semi-active methods is a good solution in these cases. A disc damper using electrorheological fluid (ERF) as damping medium is presented in this paper in detail. By applying an electric voltage to the damper, the ERF changes its state fast and reversible from low to high viscosity. The damper is applied to a light rotor system with large amplitudes like in centrifuges. The test rig is presented, too. It is essential to have a mathematical description of the ERF that is simple and as well is able to describe the most important effects of the fluid. Two material models of the ERF in shear mode are examined. The first model is a modified Bingham model. This relatively simple model calculates the shear stress in dependency of the applied voltage and the velocity in the damper. The second model is a modified Bouc-Wen model. This model can reproduce more typical effects of the ERF. The shear stress is calculated in dependency of the applied voltage, the vibration frequency and the velocity in the damper. Measurements at the test rig show the behavior of the damper operating at different excitations. The results are shown for harmonic and unbalance excitation. The influence of different damping (different voltage) on the vibration amplitudes and forces in the damper is shown and discussed. Numerical simulations of the test rig are made with both material models. It is shown that both models can describe the ERF for this application. A comparison of the experimental and numerical results leads to an evaluation of the two models.*

Keywords: *ERF, disc damper, semi active, rotor vibration*

1. INTRODUCTION

In most of the rotating machines, problems occur with vibrations during operation. These problems can often be solved by the passive methods of damping or detuning. If the conditions of the operation change in a wide range (different rotational speeds) or if the system parameters change (changes in bearing stiffness or mass), the passive methods will no longer suppress the vibrations to a satisfying level. Using active or semi-active methods is a good solution in these cases. There are several papers published that describe the use of ERF in combination with rotor systems. The first approach was using squeeze film dampers filled with ERF. First papers were published by Morishita and Mitsui (1992) and Tichy (1993). A second approach is the use of a disc damper, where the fluid is stressed in the shear mode in contrast to the squeeze mode in the squeeze film damper. The first paper using disc dampers has been published by Nikolajsen and Hoque (1990). Several works followed by Yao *et al.* (1999), Vance (2000), Wang and Meng (2003), Lim *et al.* (2005) and Zhu (2005).

2. DESIGN OF DAMPER AND TEST RIG

All works mentioned in the introduction have in common that a disc and an inner housing are mounted on the shaft by using a roller bearing. An outer housing is fixed to the ground. The housing is filled with the fluid so that the movement of the rotor is damped by the moving disc in the fluid. The bearing avoids the rotation of the disc, so only the translatory displacements are damped. The sketch on the left side of Fig. 1 shows the assembly of these dampers. One big problem is to hold the fluid inside the damper without increasing the friction of the sealing. Furthermore, in all the studies listed above, the maximum displacements were limited to very small amplitudes. Our approach inverts the whole construction to solve the mentioned problems. The sketch in the middle and the CAD drawing on the right side of Fig. 1 show the new design. The disc is now connected to the ground and the housing is mounted on the shaft by using a roller bearing. The new design allows large amplitudes (up to 5 mm) and realizes a sealing with nearly no friction loss. Only two small holes on the upper side of the damper housing must be sealed. This is done by a latex tube.

Figure 2 shows the damper and the whole test rig. Beside the damper with his frame (1), the test rig consists of an elastic shaft (2), a lumped mass in the middle of the shaft (3), two elastic bearings (4,5) at the two ends of the shaft, a motor (6) and an angular encoder (7). The frame of the damper is used to measure the fluid forces in the damper. This is done by strain gages mounted on thin aluminium sheets (8). The length between the bearings is 600 mm, the shaft has a diameter of 8 mm and the lumped mass has a weight of approximately 1 kg.

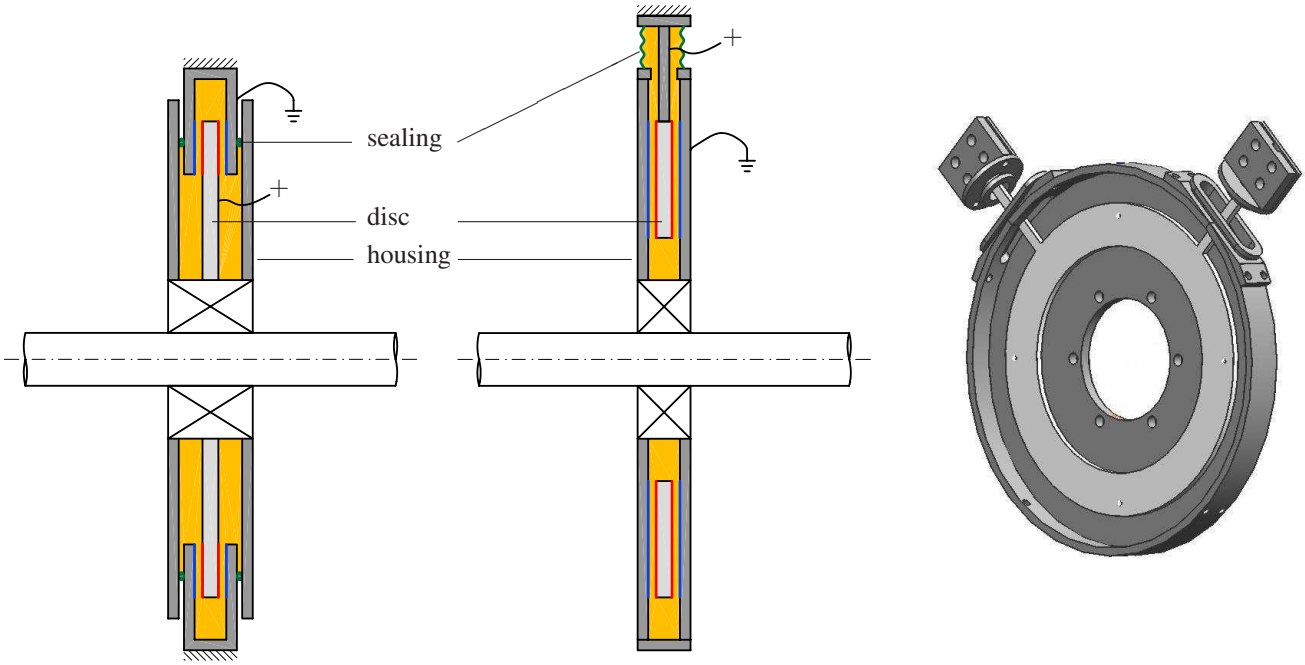

Figure 1. ERF disc damper version 1 and version 2, CAD model of opended damper (version 2)

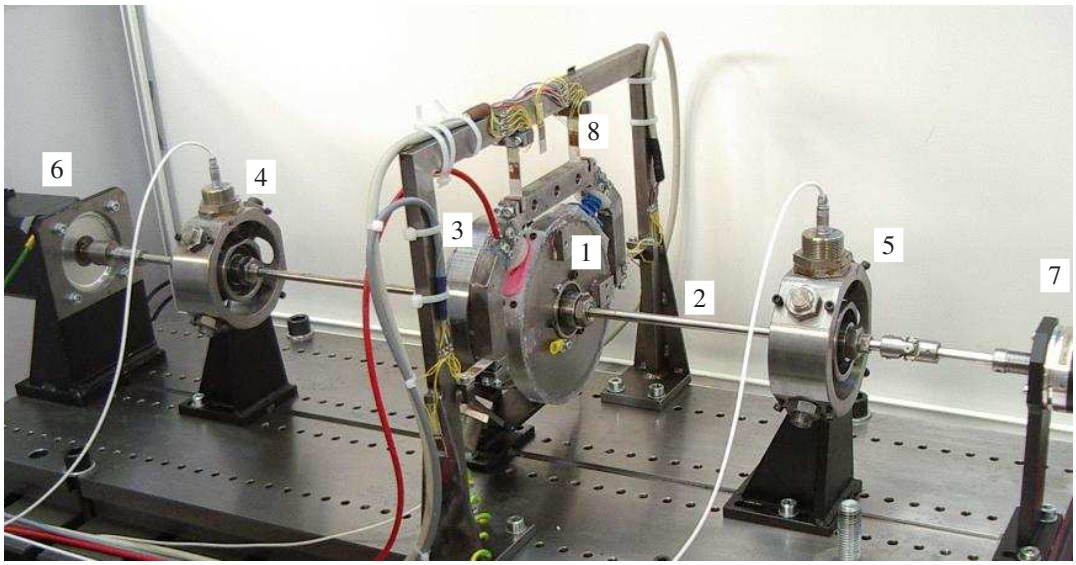

Figure 2. Rotor test rig

3. MATERIAL MODELS OF ELECTRORHEOLOGICAL FLUIDS

Electrorheological fluids (ERF) are suspensions of extremely fine non-conducting particles (normally tiny polymer spheres up to 50 μm in diameter) in an electrically insulating fluid such as silicone oil. Figure 3 shows how the particles in the ERF are spread evenly throughout the fluid when no electric field is applied (left), and the chains of particles with applied electric field (right). ERF change their apparent viscosity quickly and reversibly in response to the electric field. The response time is in the order of ms and the power requirements are very low, making ERF interesting for applications in vibration mitigation and control. The ER effect was discovered and patented by Winslow (1947, 1949).

3.1 Bingham model

As shown in Fig. 3, the particles form chains following the streamlines of the electric field. If a force is applied perpendicular to the streamlines, the chains can resist the force up to a certain level, depending on the field strength. The chains burst when the load exceeds this level and the fluid begins to flow. This behavior can easily be expressed by the

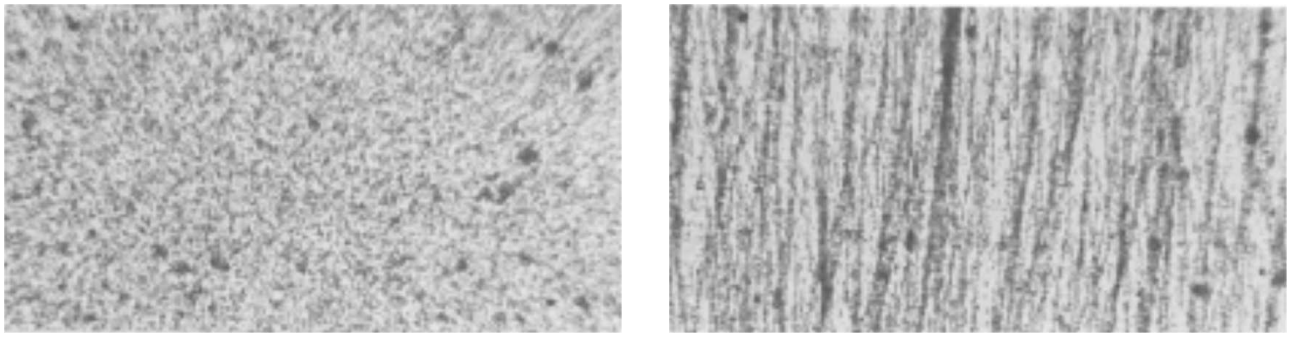

Figure 3. Particles in ERF without (left) and with applied electric field (right) (Stangroom (1983)).

Bingham model

$$\tau_{ER}(E, \dot{\gamma}) = \tau_g(E) + \nu(E)\,\dot{\gamma}\,. \tag{1}$$

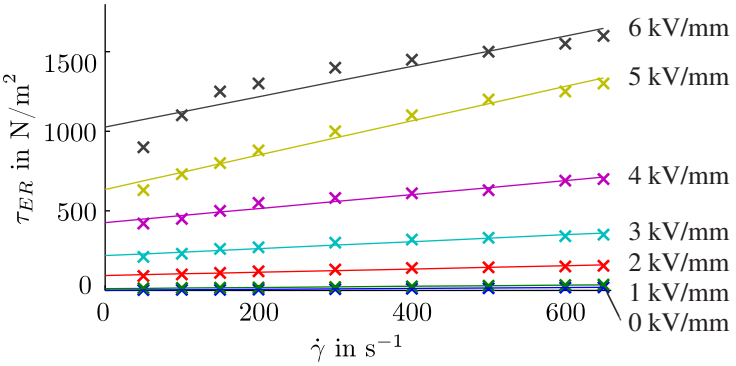

Figure 4. Shear mode measurements and linear fits for $E = 0$ kV (blue) up to $E = 6$ kV (black).

Figure 4 shows the results of some shear mode measurements done with a rheometer for field strengths from $E = 0$ kV up to $E = 6$ kV. A least square method (polyfit in MATLAB) is used to approximate the measured points by linear functions with an offset for each field strength. The results are shown in Fig. 4. The slope of the lines is equivalent to the viscosity ν and the offset is equivalent to the stress limit τ_g in Eq. (1).

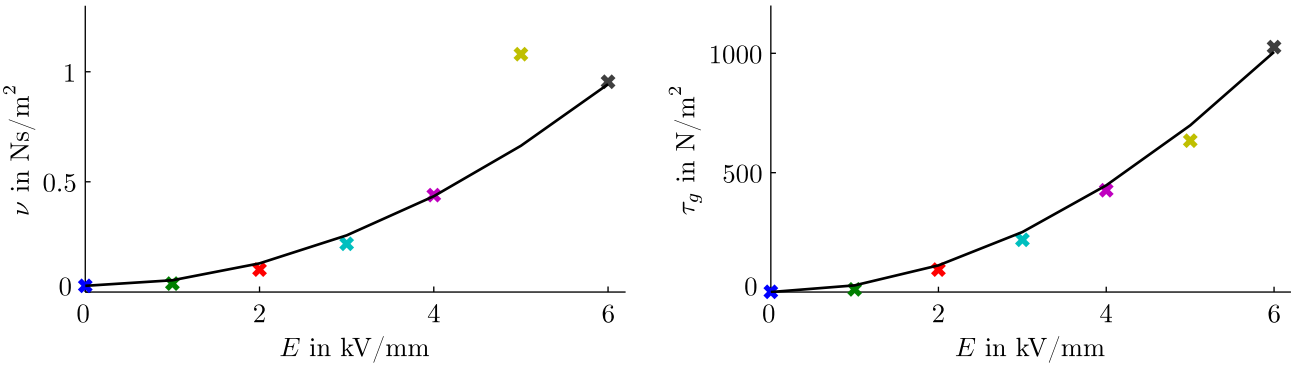

Figure 5. Dependency of viscosity ν and stress limit τ_g on the electric field strength E.

Figure 5 shows that both variables have a quadratic dependency on the electric field strength,

$$\tau_g = a_\tau E^2\,, \qquad a_\tau = 27.94\ \text{N/V}^2\,, \tag{2}$$

$$\nu = \nu_0 + a_\nu E^2\,, \qquad \nu_0 = 0.028\ \text{Ns/m}^2, \quad a_\nu = 0.025\ \text{Ns/V}^2\,. \tag{3}$$

If no voltage is applied to the fluid, it has the base viscosity ν_0. The coefficients are obtained by using the Levenberg-Marquardt algorithm for nonlinear least squares (nlinfit in MATLAB). The values for 5 kV were not considered for the

approximation, because a measurement error is supposed for this data set. For numerical simulations using the Bingham model, the shear stress is multiplied by an arctan function because the jump in the shear rate occurring in the change from negative to positive shear rates is avoided:

$$\tau_{ER}(E,\dot{\gamma}) = \left(\tau_g(E) + \nu(E)\,\dot{\gamma}\right)\frac{2}{\pi}\,\arctan\left(c\,\frac{\dot{\gamma}}{\dot{\gamma}_{max}}\right) \tag{4}$$

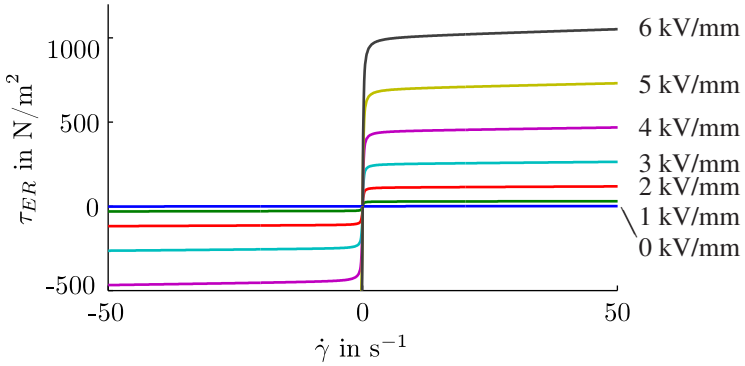

Figure 6. Bingham model using equation 4 with the approximations of the equations 2 and 3.

Figure 6 shows the final results for the Bingham model. The advantage of the Bingham model is it's simplicity. Only the three coefficients shown in Eq. (2, 3) are needed and the estimation of the parameters is unproblematic. However, the application is actually limited to slowly changing shear rates, because shear rates were constant during the estimation of the parameters.

The fluid forces F_{ER} in the damper are then calculated by multiplying the shear stress and the area A_{ER} of the damper,

$$F_{ER} = A_{ER}\,\tau_{ER}\,. \tag{5}$$

3.2 Bouc-Wen model

As mentioned before, the Bingham model is actually limited to slowly changing shear rates. Special hysteretic effects occur in the ERF when the shear rate is fast changing like in oscillations. A special test rig was designed at the Institute of Structural Dynamics, TU Darmstadt for measuring the shear stress of the fluid on a quadratic metal plate. The plate was excited in a narrow fluid gap (width: 2 mm) with a shaker. More than 500 single measurements were done and evaluated. Wen (1976) and Spencer *et al.* (1997) propose material models with distinct hysteresis behavior. Based on our measurements, the used Bouc-Wen model is extended by linear elements according to Fig. 7. The mass is constant and equal to the mass of the plate moved in the fluid. The resulting equations for the model are:

$$\begin{aligned} &F_{ER} = d_1\dot{y} \quad \text{with} \\ &\dot{y} = \frac{1}{d_0+d_1}[m\ddot{x} + d_0\dot{x} + k_0(x-y) + \alpha z] \quad \text{and} \\ &\dot{z} = \delta(\dot{x}-\dot{y}) - \gamma|\dot{x}-\dot{y}|\cdot|z|^{n-1}z - \beta(\dot{x}-\dot{y})|z|^n. \end{aligned} \tag{6}$$

Figure 8 shows one of the measurements done at our ERF test rig (black line). The excitation of the metal plate was harmonic (6 Hz, 1 mm amplitude) and the applied voltage was 6 kV so that the field strength resulted in 3 kV/mm. Using

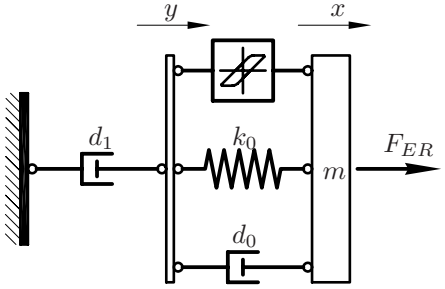

Figure 7. extended Bouc-Wen model

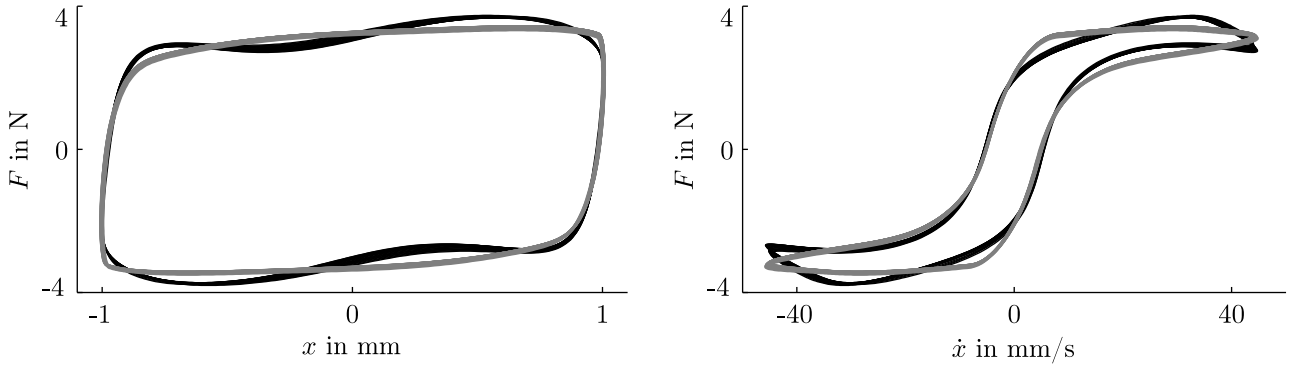

Figure 8. Measurement at ERF test rig (black) and fitted Bouc-Wen model (grey) for harmonic excitation (frequency: 6 Hz, amplitude: 1 mm, field strenth: 3 kV/mm).

the MATLAB algorithm fmincon, the Bouc-Wen model shown in Fig. 7 and described with Eq. (6) can be fitted to the measured data. The result is shown in Fig. 8 in grey. The result of the fit are the five parameters d_0, d_1, k_0, β and δ. The Bouc-Wen model reproduces the typical hysteresis that appears in the measurement. So the model seems to be a good choice for describing the ERF under harmonic excitation. The disadvantage compared with the Bingham model is the high number of model terms and the additional dependency on the frequency. For each combination of amplitude, frequency and electric field strength, the five model terms must be calculated from a measurement. The parameters change strongly so that it was not possible yet to find functions for the 5 model terms in dependency of amplitude, frequency and electric field strength. Remember that the Bingham model only has three coefficients for all possible combinations of amplitude, frequency and electric field strength. That leads to the main question of this paper: Is the simple Bingham model good enough for describing the ERF damper?

4. MEASUREMENTS

4.1 Harmonic excitation

To find an answer to this question, a set of measurements were done with the rotor test rig illustrated in Fig. 2. A harmonic force (frequency: 6 Hz) in horizontal direction was applied by a modal shaker acting on the shaft near the lumped mass. The amplifier voltage at the shaker was adjusted to keep the displacement amplitude $\widehat{y}_{ER}$ at the damper constant. The electric field strength was set to 0, 1.5 and 3 kV/mm. The time stepsize is 0.001 s and a butterworth filter is used for all signals (high pass, 0.5 Hz, order 1 / low pass, 100 Hz, order 4). Figure 9 shows the fluid forces and displacements. It can be seen, that the influence of the applied voltage on the fluid can be neglected up to 1.5 kV/mm. The viscosity is almost the same as for 0 kV/mm and the stress limit is still very low. A big difference appears when the field strength is risen up to 3 kV/mm. The force amplitudes rise significantly. In addition to the time signals the force displacement and force velocity diagrams are shown.

4.2 Unbalance excitation

For unbalance excitation, the rotor test rig was run with constant rotor speed. Three different velocities were chosen: 6 Hz (below critical speed), 9 Hz (close to critical speed) and 14 Hz (above critical speed). An unbalance mass of 26.3 g was mounted at the lumped mass at a radius of 55 mm. Figure 10 shows the results for the three measurements. The electric field strength was set to 0, 1.5 and 3 kV/mm like in the tests with harmonic excitation.

Below and near the critical speed, the displacement amplitudes can be reduced with the applied voltage. The forces in the damper are higher compared to the forces without applied high voltage. Above the critical speed, the displacement amplitudes are the same for all electric field strengths, because the amplitudes only depend on the eccentricity ε of the rotor caused by the mounted unbalance mass. The forces in the damper rise to a high level above the critical speed, even higher than in the resonance. This is caused by the viscous part of the damping force that is only proportional to the velocity. Far above critical speed, the displacements stay constant with increased rotor speed, but the increased velocity effects higher damping forces. The high voltage has no benefit above the critical speed. A control algorithm (changing the applied voltage) can improve the behavior of rotors operated at different rotor speeds. This is shown in Bauer *et al.* (2011).

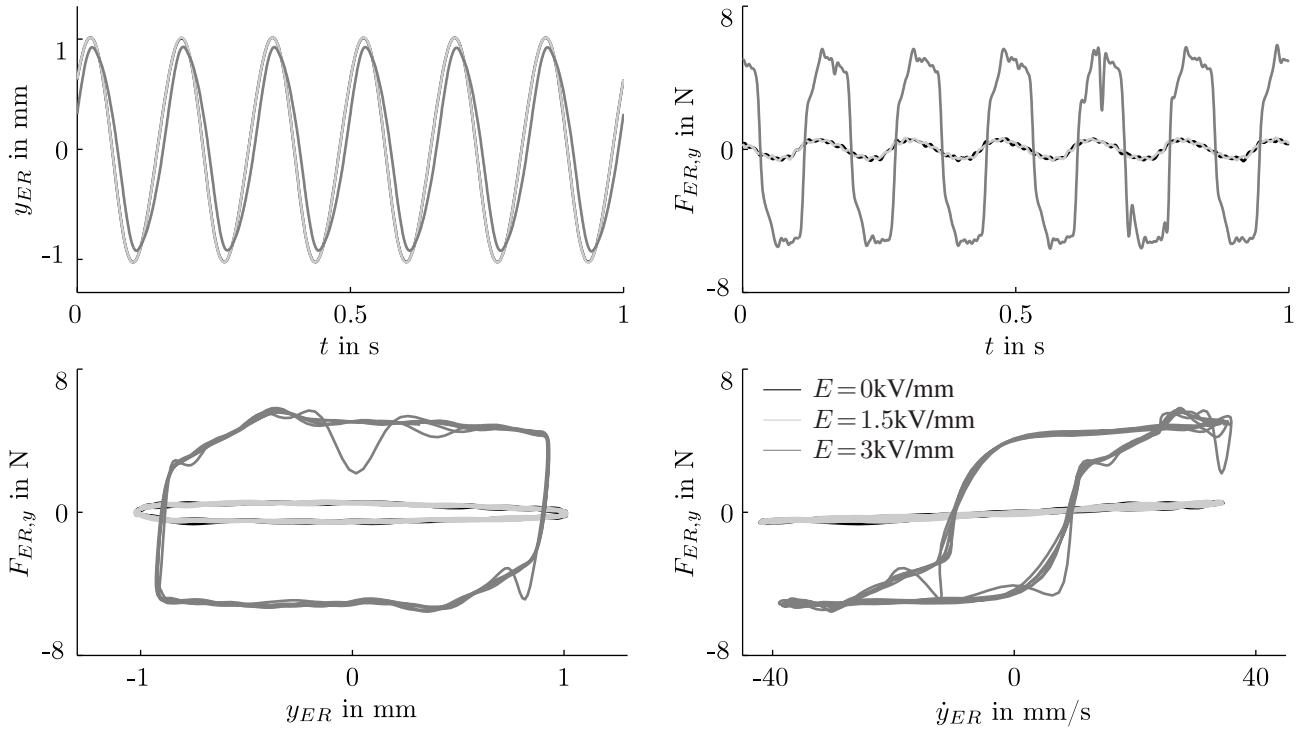

Figure 9. Measurement results at rotor test rig, 6 Hz, harmonic excitation.

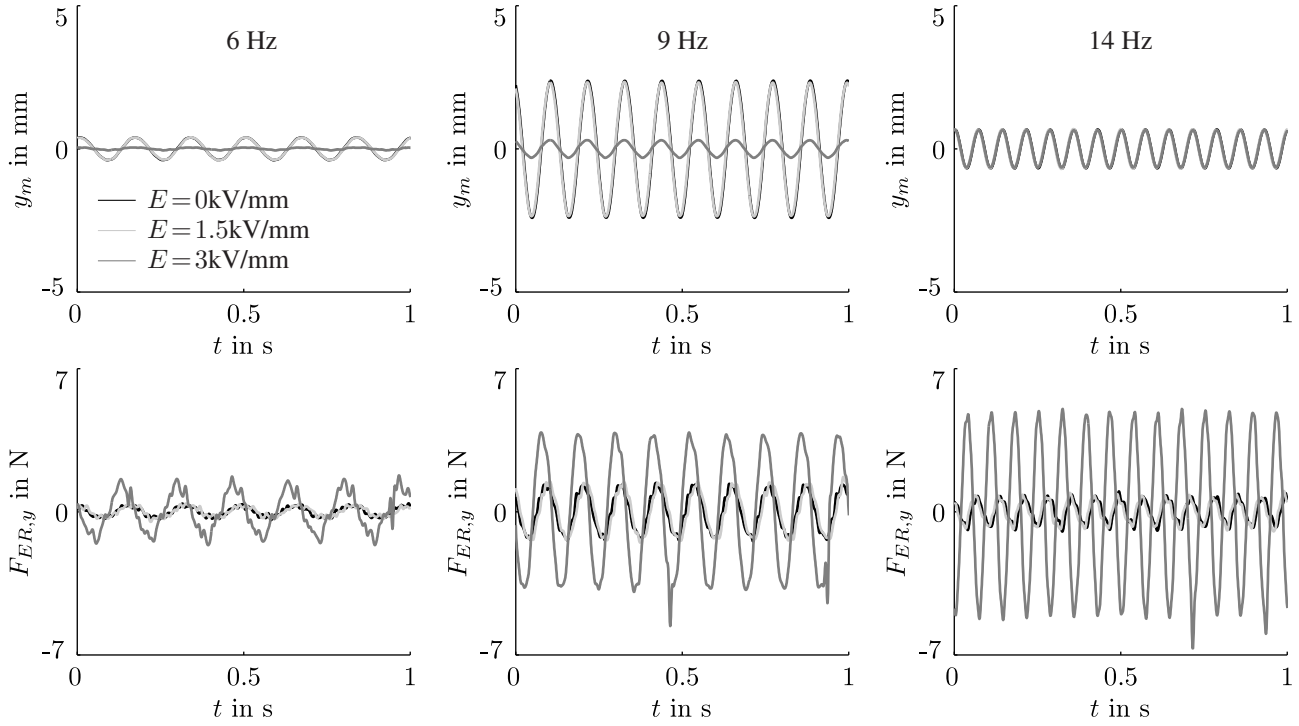

Figure 10. Measurement results at rotor test rig, 6, 9, 14 Hz, unbalance excitation.

5. SIMULATION

For the design of the damper a numerical model is needed to predict the behavior of the rotor with damper. This model consists of 4 nodes with 4 degrees of freedom on each node (2 translations, 2 rotations). Gyroscopic effects are neglected. The parameters (mass, stiffness, damping) are obtained from the real test rig. The equation of motion

$$\mathbf{M}\ddot{\mathbf{r}} + \mathbf{B}\dot{\mathbf{r}} + \mathbf{K}\mathbf{r} = \mathbf{F} - |\mathbf{F}_{ER}|\frac{\dot{r}_{ER}}{|\dot{r}_{ER}|} \tag{7}$$

is solved in the numerical model. The term on the right side of Eq. (7) represents the external forces (harmonic or unbalance excitation).

5.1 Harmonic excitation

In the numerical model of the rotor test rig, a harmonic force (frequency: 6 Hz) was applied on the node of the lumped mass. The excitation forces were chosen in the range of the measured forces of the shaker (see column 3 in Tab. 1). To make simulation and measurements comparable, the displacements are always in the range of 1 mm.

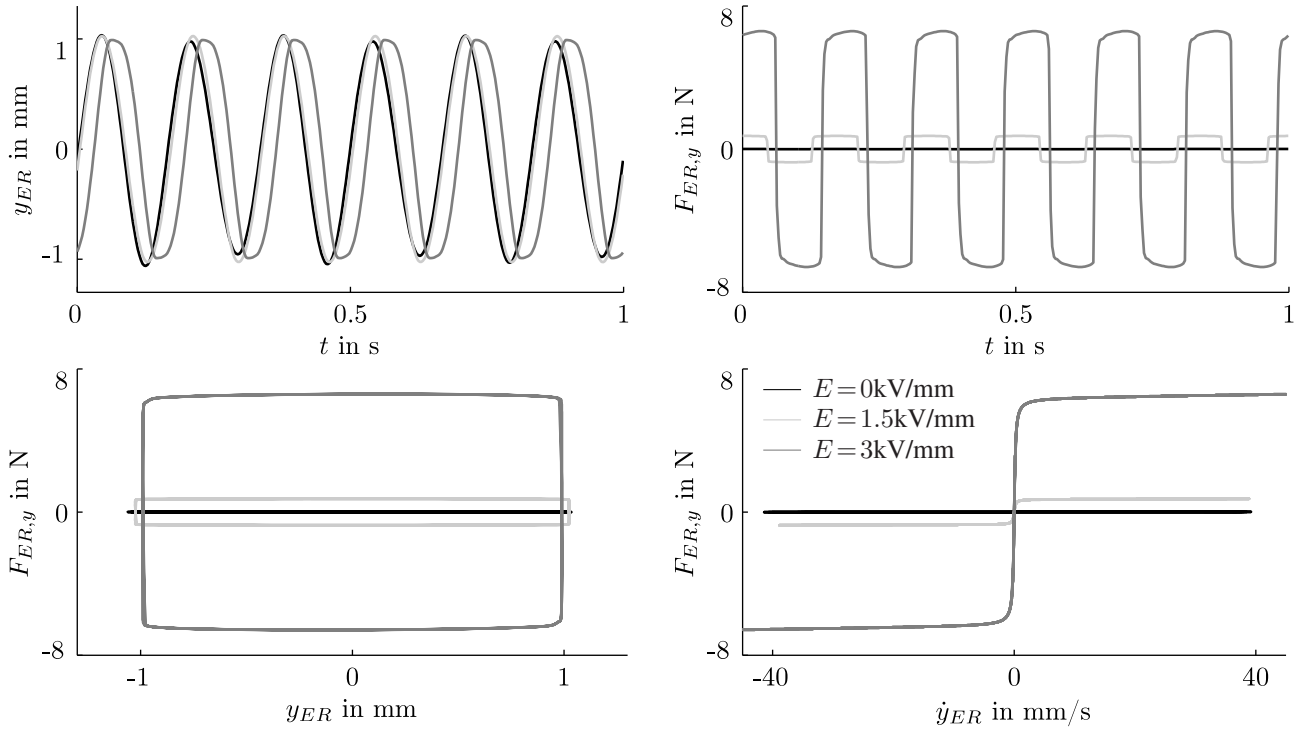

Figure 11. Simulation results, 6 Hz, harmonic excitation, Bingham Model.

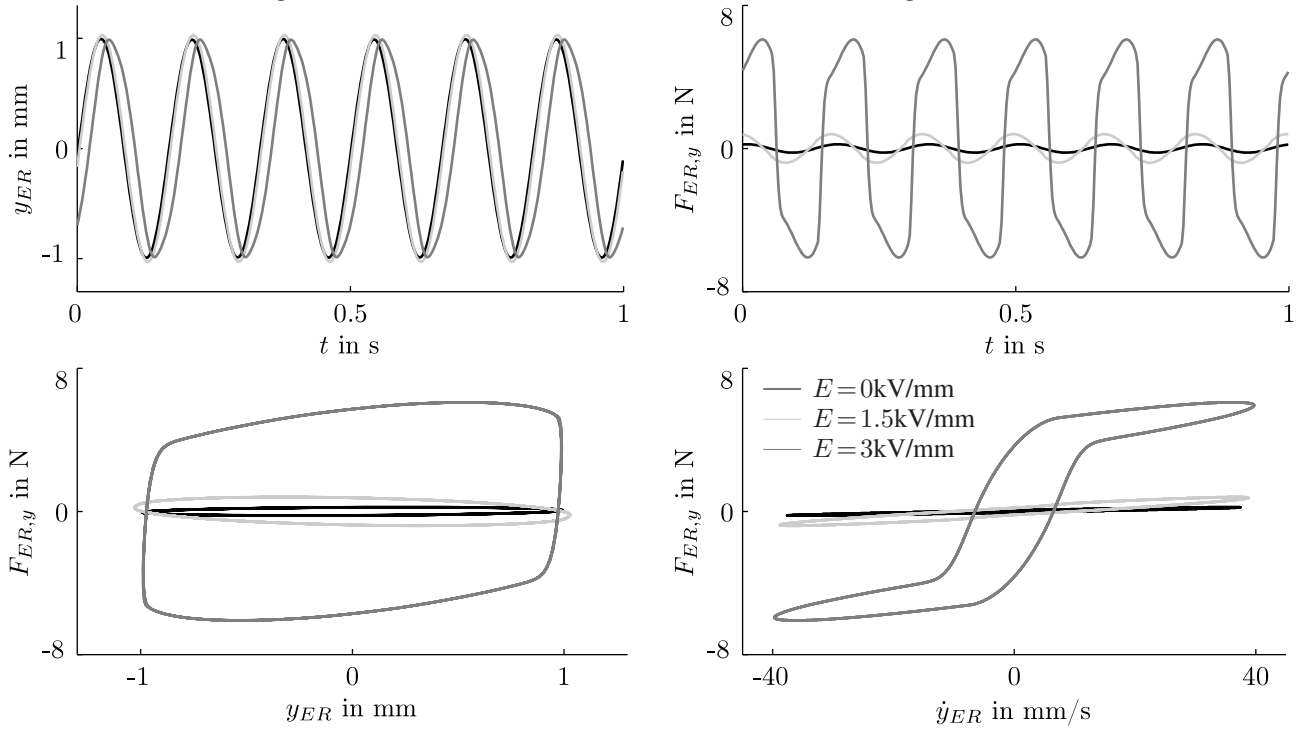

Figure 12. Simulation results, 6 Hz, harmonic excitation, Bouc-Wen Model.

Table 1. Measurement and Simulation parameters.

	E [kV/mm]	F_h [N]	$\widehat{y}_{ER}$ [mm]
Measurement	0, 1.5, 3.0	5.4, 5.4, 8.5	1, 1, 1
Bingham	0, 1.5, 4.5	6.0, 6.2, 8.7	1, 1, 1
Bouc-Wen	0, 0.5, 1.5	6.0, 6.0, 9.5	1, 1, 1

First results showed, that the fluid forces in the simulation and in the measurements were really different. Column 2 of Tab. 1 lists the adjusted electric field strengths E for the simulations. There are some reasons for the discrepancy between measurement and simulation:

1. The base viscosity in the Bingham model seems to be too low (see 0 kV line in Fig. 11), so a higher voltage was needed to get comparable results. The diagram shown in Fig. 4 was obtained from shear mode measurements in a rheometer, the temperature was 40 degrees Celsius.
2. The tests used for identifying the parameters of the Bouc-Wen model were done in a test rig with a rectangular plate. A circular plate and another gap size are used in the damper. The geometry usually effects the material model.
3. The fluid strongly sediments within a few minutes without motion. If a certain amount of particles sediments on the ground, the fluid gets "softer".

Figure 11 shows the results for the case that the Bingham model is used for describing the fluid in the damper and Fig. 12 shows the results for the Bouc-Wen model. The force displacement and force velocity diagrams show that the Bingham model of course cannot describe the hysteresis like behavior of the Bouc-Wen model, because this effect is not included in the mathematical model. The forces differ from the measurement especially in the lower voltage region.

5.2 Unbalance excitation

The same unbalance weight used in the test rig was used for the simulation, too. The field strengths were chosen as listed in Tab. 1. Instead of 9 Hz like in the measurement, 8.7 Hz were chosen for the simulation, because the displacement amplitudes were higher compared to the measured data. The main reason for that is that the numerical model has an exact critical speed of 9 Hz and that the real test rig slightly differs from the model. Additionally, the test rig was not run directly in the resonance. Both models show a similar behavior. The main effects described in chapter 4.2 are reproduced by both models.

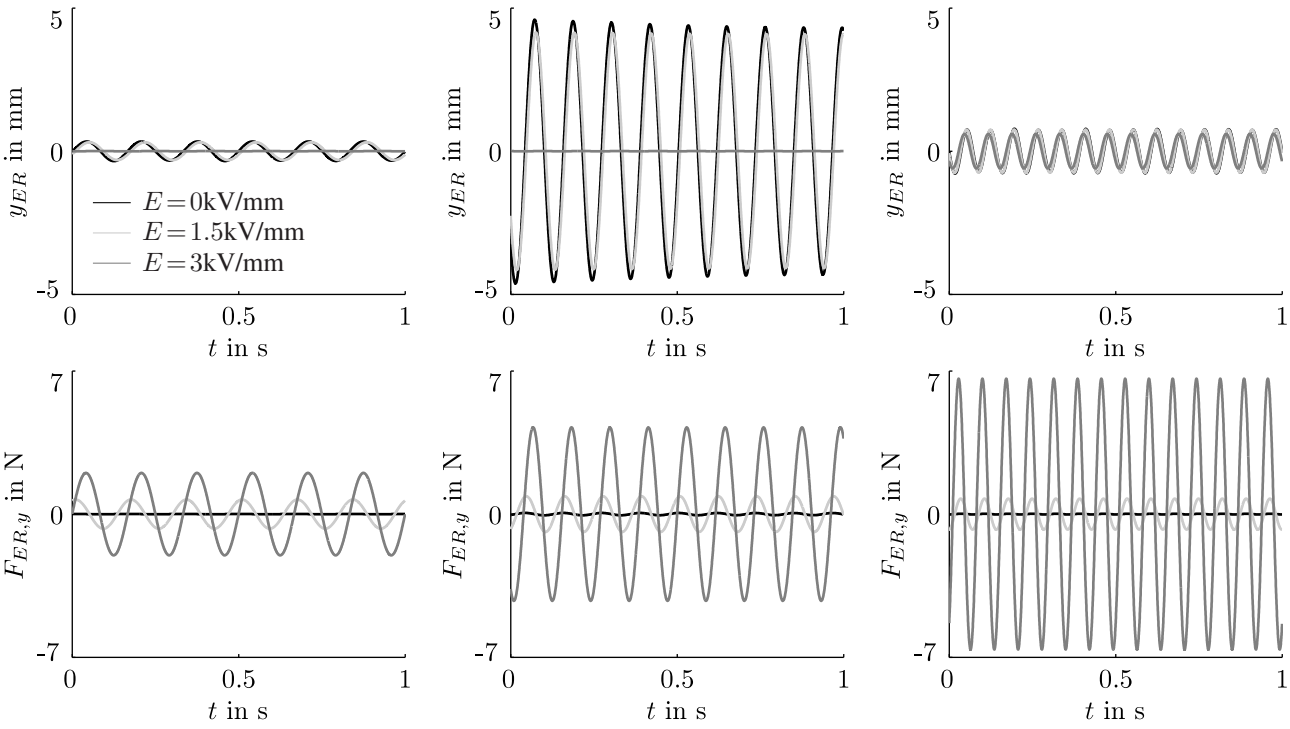

Figure 13. Simulation results, Bingham model, 6, 8.7, 14 Hz, unbalance excitation.

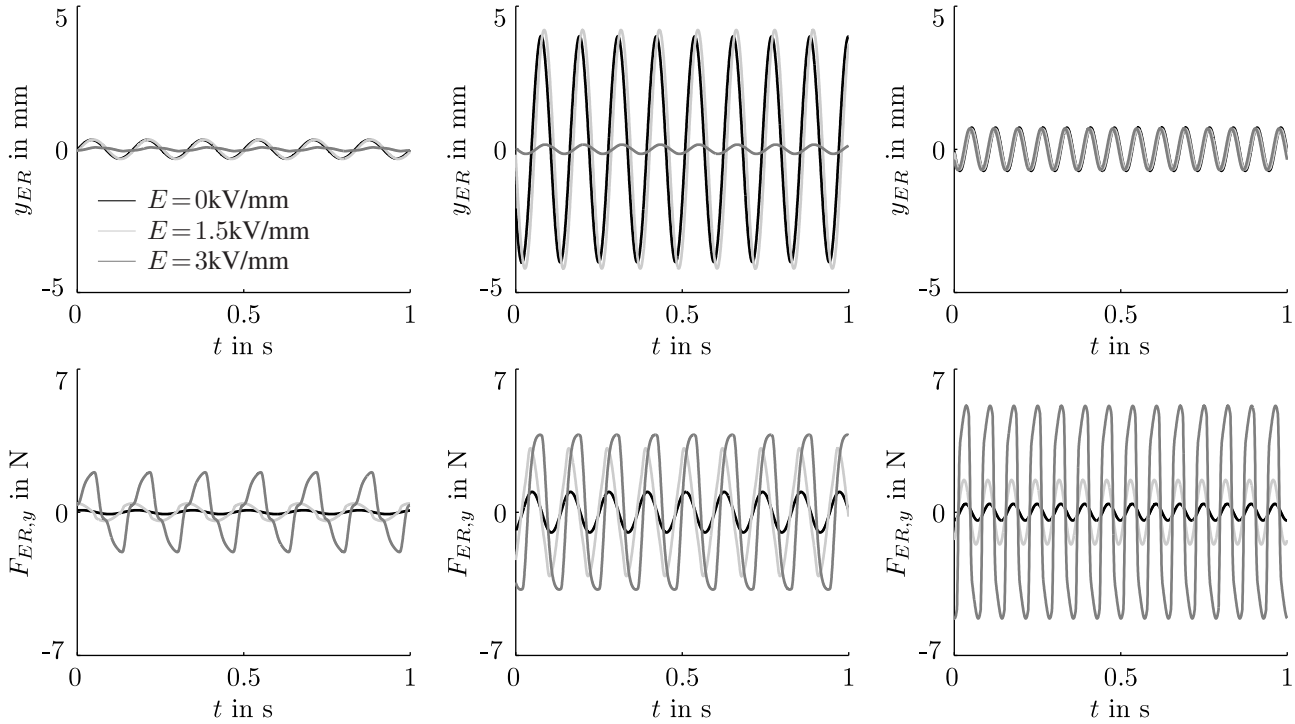

Figure 14. Simulation results, Bouc-Wen model, 6, 8.7, 14 Hz, unbalance excitation.

6. COMPARISON AND CONCLUSION

The Bingham and the Bouc-Wen model were tested with harmonic and unbalance excitation. Under harmonic excitation, the damper stands still and accelerates again. Hysteresis effects occur in this motion that only the Bouc-Wen model can reproduce. However, the global effect of influencing the force and displacement dependent of the high voltage can be reproduced by both models. Under unbalance excitation, the damper moves continuously. Both models can describe the behavior quite well. Because of its simplicity, the Bingham model is proposed to be used at least for the simulation of unbalance excited vibrations of a rotor with constant speed or in a slow run-up. However, there are still some points to be examined, because the applied field strength was different in the shown simulations and measurements. In further steps, the parameters of the two material models will be obtained from measurements at the damper (isolated from the rotor) so that differences in the geometry can be eliminated.

7. REFERENCES

Bauer, J., Köhl, W., Markert, R. and Cavalca, K.L., 2011. "ERF-Schwingungsdämpfer für leichte Rotorsysteme mit großen Amplituden". In *9. internationale Tagung Schwingungen in Rotierenden Maschinen, ISBN 978-3-9814163-0-5*. Darmstadt, Germany.

Lim, S., Park, S.M. and Kim, K.I., 2005. "AI vibration control of high-speed rotor systems using electrorheological fluid". *Journal of Sound and Vibration*, Vol. 284, pp. 685–703.

Morishita, S. and Mitsui, Y., 1992. "Controllable squeeze film damper (an application of electro-rheological fluid)". *Journal of Vibration and Acoustics*, Vol. 114(2), pp. 354–357.

Nikolajsen, J.L. and Hoque, M.S., 1990. "An electroviscous damper for rotor application". *Journal of Vibration and Acoustics*, Vol. 112, pp. 440–443.

Spencer, B.F., Dyke, S.J., Sain, M.K. and Carlson, J.D., 1997. "Phenomenological model of a magnetorheological damper". *Journal of Engineering Mechanics*, Vol. 123, pp. 230–238.

Stangroom, J.E., 1983. "Electrorheological fluids". *Physics in Technology*, Vol. 14, p. 290.

Tichy, J.A., 1993. "Behavior of a squeeze film damper with an electrorheological fluid". *STLE Tribology Transactions*, Vol. 36(1), pp. 127–133.

Vance, J.M., 2000. "Experimental measurements of actively controlled bearing damping with an electrorheological fluid". *Journal of Engeneering for Gas Turbines and Power*, Vol. 122, pp. 337–344.

Wang, J. and Meng, G., 2003. "Experimental study on stability of an MR fluid damper-rotor-journal bearing system". *Journal of Sound and Vibration*, Vol. 262, pp. 999–1007.

Wen, Y.K., 1976. "Method of random vibration of hysteretic systems". *Journal of Engineering Mechanics Devision*, Vol. 102, pp. 249–263.

Winslow, W.M., 1947. "Method and means for translating electrical impulses into mechanical force".

Winslow, W.M., 1949. "Induced fibration of suspensions". *Journal of Applied Physics*, Vol. 20, pp. 1137–1140.

Yao, G.Z., Qiu, Y., Meng, G., Fang, T. and Fan, Y.B., 1999. "Vibration control of a rotor system by disk type electrorheological damper". *Journal of Sound and Vibration*, Vol. 219(1), pp. 175–188.

Zhu, C., 2005. "A disk-type magneto-rheological fluid damper for rotor system vibration control". *Journal of Sound and Vibration*, Vol. 283, pp. 1051–1069.

8. Responsibility notice

The authors are the only responsible for the printed material included in this paper.